Final Report

Project Title: Effect of deferiprone on brain iron distribution of β-thalassemic mice using Magnetic Resonance Imaging (MRI)

By Paranee Yatmark

April 2018

Contract No: MRG5980059

Final Report

Project Title: Effect of deferiprone on brain iron distribution of β-thalassemic mice using Magnetic Resonance Imaging (MRI)

Asst. Prof. Dr. Paranee Yatmark
Faculty of Veterinary Science, Mahidol University

Project Granted by the Thailand Research Fund

Abstract

Project Code : **MRG5980059**

Project Title : **Effect of deferiprone on brain iron distribution of β-thalassemic mice using Magnetic Resonance Imaging (MRI)**

Investigator : **Dr. Paranee Yatmark**
Department: Pre-clinic and Applied Animal Science, Faculty of Veterinary Science, Mahidol University

E-mail Address : **paranee.yat@mahidol.edu**

Project Period : **May 2559-April 2561**

Executive summary:

Brain iron overload is a chronic and slow progression that plays an important role in the pathogenesis of neurodegenerative disorders. Magnetic resonance imaging (MRI) is a useful non-invasive tool for determining liver iron content, but not proven to be adequate for evaluating brain iron overload. This study was to evaluate the usefulness of MRI-derived parameters to determine brain iron concentration in β-thalassemic mice and the effects of membrane permeable iron chelator, deferiprone. Eighteen β-thalassemic mice underwent 1.5 T MRI of the brain and iron level was quantified using T2* value with cardiovascular magnetic resonance (CMR) software. The results showed that the mean brain T2* values 28.51±4.53 ms for β-thalassemic mice. For the iron overloaded thalassemic mice, brain T2* values decreased to 9.80±0.94 ms, with correlated with iron overload status of the animals. In addition, brain T2* values increased

in the group of the treatment of deferiprone 17.87±3.85ms. Additionally, we found that brain iron content was correlation significance with brain T2* values in β-thalassemic mice. Our results may useful to understand brain pathology in iron overload. Moreover, data could lead to earlier diagnosis, assist in following disease progression, and the benefits of iron chelation therapy.

Keywords: brain iron overload, brain pathology, deferiprone, β-thalassemic mice, Magnetic resonance imaging

บทคัดย่อ

รหัสโครงการ : MRG5980059

ชื่อโครงการ : **การศึกษาผลของยาขับเหล็กต่อการกระจายตัวของเหล็กในสมองของหนูที่เป็นโรคธาลัสซีเมียโดยใช้เครื่องตรวจวินิจฉัยด้วยคลื่นแม่เหล็กไฟฟ้า**

ชื่อนักวิจัย : **ผศ.ดร.ปารณีย์ ญาติมาก**

ภาควิชาปรีคลินิกและสัตวศาสตร์ประยุกต์ คณะสัตวแพทยศาสตร์

มหาวิทยาลัยมหิดล

E-mail Address: paranee.yat@mahidol.edu

ระยะเวลาโครงการ: **พฤษภาคม 2559 – เมษายน 2561**

บทสรุป:

ภาวะเหล็กเกินที่เกิดขึ้นในสมองส่งผลต่อการเกิดความผิดปกติที่สมองอย่างช้าๆจนเรื้อรัง ซึ่งมีบทบาทสำคัญที่ทำให้เกิดโรคทางระบบประสาทตามมาได้ เครื่องตรวจวินิจฉัยด้วยคลื่นแม่เหล็กไฟฟ้า เป็นเทคนิคหนึ่งที่ไม่ก่อให้เกิดความเจ็บปวด สามารถตรวจวัดระดับเหล็กในตับได้ แต่ยังมีข้อมูลไม่เพียงพอสำหรับการประเมินระดับเหล็กเกินในสมอง การศึกษานี้ได้ประเมินดูการใช้เครื่องตรวจวินิจฉัยด้วยคลื่นแม่เหล็กไฟฟ้า ในการวัดระดับเหล็กในสมองในหนูที่เป็นโรคธาลัสซีเมียและดูผลของยาขับเหล็ก ยาดีเฟอริโพรน หนูที่เป็นโรคธาลัสซีเมีย 18 ตัว

ได้วัดระดับเหล็กในสมองด้วยเครื่องตรวจวินิจฉัยด้วยคลื่นแม่เหล็กไฟฟ้า และใช้โปรแกรม cardiovascular magnetic resonance (CMR) ช่วยในการคำนวณค่า T2* ผลการศึกษาพบว่าค่าเฉลี่ย 28.51±4.53 ms ในสมองของหนูที่เป็นโรคธาลัสซีเมียอยู่ที่ 9.80±0.94 ms ในหนูที่ได้รับเหล็กเกิน พบค่าเฉลี่ย 17.87±3.85 ms ซึ่งลดลงจากหนูที่ไม่ได้รับเหล็กเกิน และสัมพันธ์กับระดับเหล็กที่เพิ่มมากขึ้น ยิ่งไปกว่านั้นในกลุ่มที่ได้รับยาขับเหล็ก พบว่าค่าเฉลี่ย T2* เพิ่มขึ้น ซึ่งหมายถึงระดับเหล็กที่ลดลงอย่างมีนัยสำคัญทางสถิติ นอกจากนี้ได้วัดระดับเหล็กในสมองของหนูที่เป็นโรคธาลัสซีเมีย พบว่ามีความสัมพันธ์กับค่าเฉลี่ย T2* ที่ได้จากเครื่องตรวจวินิจฉัยด้วยคลื่นแม่เหล็กไฟฟ้า ผลการศึกษานี้อาจจะเป็นประโยชน์ต่อการศึกษาพยาธิสภาพของสมองที่มีภาวะเหล็กเกิน ข้อมูลที่ได้นำไปสู่การช่วยวินิจฉัยระดับเหล็กในสมอง ติดตาม พยากรณ์การเกิดโรคทางสมอง และเป็นประโยชน์ต่อการรักษาด้วยยาขับเหล็กต่อไป

คำสำคัญ ภาวะเหล็กเกินในสมอง พยาธิสภาพของสมอง ยาดีเฟอริโพรน หนูธาลัสซีเมีย เครื่องตรวจวินิจฉัยด้วยคลื่นแม่เหล็กไฟฟ้า

Final report content:

Abstract:

Brain iron overload is a chronic and slow progression that plays an important role in the pathogenesis of neurodegenerative disorders. Magnetic resonance imaging (MRI) is a useful non-invasive tool for determining liver iron content, but not proven to be adequate for evaluating brain iron overload. This study was to evaluate the usefulness of MRI-derived parameters to determine brain iron concentration in β-thalassemic mice and the effects of membrane permeable iron chelator, deferiprone. Eighteen β-thalassemic mice underwent 1.5 T MRI of the brain and iron level was quantified using T2* value with cardiovascular magnetic resonance (CMR) software. The results showed that the mean brain T2* values 28.51±4.53 ms for β-thalassemic mice. For the iron overloaded thalassemic mice, brain T2* values decreased to 9.80±0.94 ms, with correlated with iron overload status of the animals. In addition, brain T2* values increased in the group of the treatment of deferiprone 17.87±3.85ms. Additionally, we found that brain iron content was correlation significance with brain T2* values in β-thalassemic mice. Our results may useful to understand brain pathology in iron overload. Moreover, data could lead to earlier diagnosis; assist in following disease progression, and the benefits of iron chelation therapy.

Keywords: brain iron overload, brain pathology, deferiprone, β-thalassemic mice, Magnetic resonance imaging

Introduction

In the CNS, iron plays an important role in many biological processes including oxygen transportation, mitochondrial respiration, neurotransmitter synthesis and myelin production (Crichton et al., 2009; Mounsey and Teismann, 2012). However, if iron is not correctly controlled, it can be damaging to neurons and contributes to the pathogenesis of several neurological diseases. Brain iron accumulation is an initial cause of neuronal death, has been reported in neurodegenerative diseases and inflammatory central nervous system including Parkinson's disease, Alzheimer diseases, and neuroferritinopathy (Brass et al., 2006; Berg and Youdim, 2006; Stankiewicz et al., 2007; Duce et al., 2010). The cause of iron metabolism for disorders in the brain remains indescribable. Increased iron deposition may be attributable to local changes of the normal iron-regulatory systems (Qian and Shen, 2001; Ke and Ming Qian, 2003). Previous studied shown iron overload accelerates cognitive impairment in transgenic mice model of Alzheimer's disease (Becerril-Ortega et al., 2014).

Patients with transfusional iron overload begin to develop pituitary iron overload in the first decade of life. Pituitary iron overload and volume loss were independently predictive of hypogonadism (Noetzli et al., 2012). Iron toxicity in the pituitary gland, primarily affects the gonadotropin-secreting cells, and hypogonadotropic hypogonadism is a frequent abnormality in thalassemic patients (Modell et al., 2000, Olson et al., 1987, Brittenham et al., 1982). In thalassaemic patients, hypogonodotropic hypogonadism resulting from pituitary dysfunction due to iron overload remains the most frequent complication even among adequately chelated (Jensen et al., 1997). During adolescence, anterior pituitary’s intact function is importance as it regulates growth and sexual maturation, directly affecting quality of life in younger patients with β-thalassaemia major. Previous studied, abnormal increase of iron only occurred in some specific

regions of the brain of patients with neurodegenerative disorders (Lee et al., 2006). Brain iron overload associated with worse cognitive performance in obese subjects (Blasco et al., 2014). Neurodegeneration that results from iron toxicity can lead to apoptosis and ferroptosis, an iron-specific form of non-apoptotic cell death (Ott et al., 2007, Dixon and Christoff, 2012). However, it is not clearly that increased iron deposition may be contributed with the pathogenesis of these diseases.

Magnetic resonance imaging (MRI) has long been considered a useful noninvasive tool for evaluating iron overload in organs (Brittenham et al., 2003). In the human brain over the last two decades, as iron deposition in tissues lead to signal changes in T2*-weighted MR images (Bartzokis et al., 1993). MRI for iron overload was first used in hemochromatosis, one of the most frequent diffuse liver diseases. Since then MRI has widely replaced biopsies when investigating liver iron overload. It has been mainly used to evaluate brain iron accumulation in multiple sclerosis (Khalil et al., 2011) and neurodegenerative diseases including Alzheimer's and Parkinson's disease (Bartzokis et al., 2000; Brass et al., 2006; Thomas et al., 1993).

Therefore, there are few published data with reference to the brain iron accumulation in patients with β-thalasemia major (Argyropoulou et al., 2007). Literature concerning iron distribution in the brain using MRI is limited and with only one study involving series of thalassemia patients using MRI. This study showed significantly higher R2 values in the cortex, the putamen and the caudate nucleus in patients than in normal subjects (Metafratzi et al., 2001). The T2* method, although indirectly validated, seems to be well correlated to clinical data (Anderson et al., 2001).

Moreover, there is no report on brain iron accumulation in β-thalassemic mice using MRI technique. Therefore, the present study aimed to investigate the iron accumulation in the brain of

β-thalassemic mice using MRI technique. The results of MRI may demonstrate the distribution and relative amount of iron in different brain regions. The results will be correlated with iron overload status of the animals. Moreover the effects of membrane permeable iron chelator, deferiprone will be studied. The results from this study may help to understand brain pathology in iron overload and the benefits of iron chelation therapy.

Literature review

1. Brain iron metabolism

Iron is an essential trace element vital for normal brain metabolism (Altamura and Muckenthaler, 2009). Although heme-bound iron represents approximately 2-3 of all iron in the body, brain iron is primarily stored in the proteins ferritin and hemosiderin, which help as a defense beside harmful iron deficiency or iron overload (Bothwell, 1995). Iron enters the endothelial cells of the blood brain barrier as a low molecular weight complex, or individually as non-transferrin-bound iron or transferring receptor mediated endocytosis of transferrin (Moos et al., 2007, Leitner and Connor 2012). Astrocytes are preferably located to take up iron from the circulation and distribute it to other cells in the CNS. Iron can be stored as ferritin in astrocytes and exported by a mechanism that involves ferroportin and ceruloplasmin (Dringen et al., 2007). Neurons and microglia can influx iron via transferrin receptor and efflux iron via ferroportin (Huang et al., 2006). Iron homeostasis depends on the balance between iron uptake and iron release in mammalian cells. Divalent Metal Transporter 1 (DMT1) and Transferrin receptor 1 (TfR1) are key transporters for iron uptake in the brain (Ke and Qian, 2003).

2. Brain iron overload

Brain iron accumulation occurring from the absence of functional multicopper oxidase ceruloplasmin in aceruloplasminaemia impairs cellular iron efflux. In iron overloaded areas of the brain was presented in neurons and microglia (Rouault, 2013; Dusek and Schneider 2012). The excessive iron accumulation results from the inability of astrocytes to mobilize their iron to be used by neurons (Madsen and Gitlin 2007). Increased iron accumulations have also been detected in chronic hemorrhage, cerebral infarction, anemia, thalassemia, and hemochromatosis (Haacke et al., 2005). Both the physiological role and reasons for the distribution patterns of non-heme iron are still not clearly (Gerlach et al., 1994; Ke and Qian, 2003; Schenck and Zimmerman, 2004). At the cellular level, more iron staining is observed in the microglia and astrocytes of the cortex, cerebellum, hippocampus, basal ganglia and amygdale. Iron accumulation in microglia might stimulate the activation of these cells in the neuroinflammatory processes (Connor et al., 1990).

Previous study demonstrated that increased iron deposition in the anterior pituitary gland is the cause of hypogonadotropic hypogonadism (HH) and growth hormone deficiency (Bergeron and Kovacs 1978; Oerter et al., 1993). Iron accumulates in all cell types of the adenohypophysis, but preferentially in the gonadotropin-secreting cells. Gonadotropin cell death due to iron toxicity is probably the cause of the decreased pituitary gland height observed in thalassemia patients with HH (Argyropoulou et al., 2000). Hypogonadism occurs in approximately half of thalassemia patients and has long-term consequences for fertility, bone density, and quality of life (Borgna-Pignatti et al., 2004, Vogiatzi et al., 2009). Severe iron deposition is associated with decreased response to gonatropin releasing hormone challenge (Argyropoulou et al., 2000). The degree of pituitary iron overload has been evaluated by

magnetic resonance and found in thalassemic patients with hypogonadotropic hypogonadism than in those without pituitary dysfunction (Fischer 1998, Brasch et al., 1984).

3. Tissue iron by MRI techniques

MRI uses the magnetic properties of the human body to provide images of any tissue. Hydrogen nuclei are a principal component of body tissues in water and lipid molecules and produce a magnetic field that can interact with an external magnetic field. Several MR-based techniques have been proposed for detecting and quantifying iron in the tissue non-invasively (Haacke et al., 2005). Tissue iron is detected indirectly by the effects on relaxation times of ferritin and hemosiderin iron interacting with hydrogen. In practice, anatomical visualization of deep gray matter nuclei with elevated iron load in vivo has been demonstrated stimulating with conventional MR imaging (Deoni and Catani, 2007). Quantitative MRI techniques, such as mapping of the relaxation rate R2* (1/T2*), represent an indirect measure of iron, which has recently been confirmed in a postmortem study (Langkammer et al., 2010). These techniques also assist in vivo studies and offer the opportunity to correlate regional iron concentrations in tissue to clinical phenotypes (Wood et al., 2005).

Recently, T2* MRI has developed as the technique of choice for non-invasive quantification of hepatic and myocardial iron overload. It shows good sensitivity when compared with the hepatic iron concentration of liver biopsies, and cardiac T2* correlates inversely with cardiac iron concentration (Anderson et al., 2001). MRI has been used to evaluate pituitary siderosis and shows significant correlation with serum ferritin (Christoforidis et al., 2006). However, many studies have shown that body tissues have different iron deposition kinetics (Anderson et al., 2001, Wood et al., 2007, Noetzli et al., 2008). It can generate images at various

echo times to vary the contrast among different organs. All organs darken with increasing echo time, but those containing iron darken more rapidly. T2* represents the echo time necessary for a tissue to become twice as dark. It may be thought of as a half-life, with small values representing rapid signal loss. Alternatively, image darkening can be expressed by R2*, its rate of darkening (Wood et al., 2005, Carpenter et al., 2011). It has been most widely used in patient with thalassemia major, but it is also essential in thalassemia intermediate, sickle cell disease, and myelodysplasia (Wood et al., 2008; Fragasso et al., 2011).

4. Iron chelation for brain iron overload

Iron chelation as a potential therapy for removing excess iron from specific brain regions affected by neurodegenerative diseases has expected much consideration. To be effective, an iron chelator should be able to penetrate both cellular membranes and the blood brain barrier, and be able to remove chelatable iron from the site of accumulation or to transfer it to other biological proteins, such as circulating transferring (Boddaert et al., 2007). Chelation therapy has been reported to provide improvements, especially with deferiprone, and particularly for other neurodegeneration with brain iron accumulation diseases (Chinnery et al., 2007). Previous study suggested that the form of iron chelated was a labile iron pool, with iron possibly being bound to enzymes, such as hydroxylases, and to ferritin (Boddaert et al., 2007). However, iron chelator can remove iron from conjugated iron containing proteins and molecules is unknown; the chelators in clinical use were developed to remove iron from ferritin and haemosiderin in clearly iron overloaded tissues, such as the liver, heart, and spleen.

MRI is a likely technique to assess the efficacy of a treatment, although the quantitative accuracy of MRI might be dependent on the type and molecular distribution of iron (Hocq et al.,

2009). Recently, cardiac and liver iron estimates by MRI have become the primary outcome measures for clinical studies of iron chelation therapy (Pennell et al., 2006, Wood et al., 2010). However, few studies evaluating iron distribution in the brain using MRI. The only one study assessing iron in the brain of thalassemia patients by MRI showed significantly higher R2 values in the cortex, the putamen and the caudate nucleus in patients than in controls (Metafratzi et al., 2001). Quantitative information of iron content is meaning for early clinical diagnosis, monitoring of treatment, and disease progression (Utter and Basso, 2008).

In the experiment animal model of iron dextran loading β-thalassemic mice (Yatmark et al., 2014; 2015). These model showed heavy iron accumulation in the liver, heart and found increased iron accumulation in the brain. In addition, our model could attenuate tissues damage by treatment with the iron chelators, deferoxamine (DFO) and deferiprone (L1). Therefore, this study aim to investigate the brain iron accumulation in β-thalassemic mice using magnetic resonance imaging (MRI) and the effects of deferiprone was also evaluated. Moreover, measurement of brain T2* by MRI is a noninvasive direct method that has been developed for detecting and quantifying iron levels and might be reduce the risk of future neurodegenerative disease in thalassemia patients. Our results could be a supportive data for beneficial use of iron chelators in concerting about impairment brain complications in thalassemia and other diseases.

Objectives

1 To optimize brain MRI protocols to study the distribution of iron in the brain of iron overloaded β-thalassemic mice

2 To correlate brain iron deposition by MRI data and iron content with those of liver of β-thalassemic mice

3 To investigate the effect of deferiprone on brain iron deposition in iron overloaded β-thalassemic mice using MRI

Research methodology

Animals

Male and female heterozygous β-globin knockout mice (muβth3/+, BKO) 7 weeks of age and weighing 17-25 g were obtained from the Thalassemia Research Center, Institute of Science and Technology for Research and Development, Mahidol University, Thailand. β-globin gene knockout was produced by heterozygous deletion of both major and minor on chromosome 7 of mice, leading to β-globin deficiency. As a result, mice developed pathological and clinical signs resemble β-thalassemia intermedia in human (Yang et al. 1995, Jamsai et al. 2006). Mice were acclimatized for 1 week before the experiments and were housed under conventional sterile conditions. The rodent diet (082G/15) and water were provided ad libitum. The temperature and humidity were maintained at 25±2°C and 60±5%, respectively, and the animals were kept on a 12 h light/dark cycle.

Experimental design

BKO mice will be divided into 3 groups: group A: control group and group B: iron overloaded with iron dextran 5 doses and group C: iron overloaded with iron chelator. Iron overload was induced by iron dextran (Sigma, St. Louis, MO) intraperitoneal (i.p.) injection at a dose of 20 mg iron/mouse for vary doses a maximum period of 5 days for a total iron administration of 100 mg/mouse. BKO mice will be examined brain and liver iron concentration and analyzed using MRI as previously described (Grabill et al., 2003). The MRI protocol and method of MRI analysis will be modified to obtain the best result of iron distribution.

To investigate the effect of iron chelator (deferiprone, L1) on brain and liver iron deposition by MRI, iron content and histopathology

BKO mice will be divided into 3 groups (6 mice/groups): group A: control group (0.9 % NaCl), group B: iron overloaded with iron dextran and group C: deferiprone treatment (80 mg/kg) after iron overload. The dose of L1 from our previous studied (Yatmark et al., 2014).

Controls group will be i.p. injected with 0.9% NaCl with the same schedule of the treated groups. Three days after the last dose of iron dextran, iron loaded mice will be i.p. injected with 80 mg/kg/day deferiprone (L1, The Government Pharmaceutical Organization, Bangkok, Thailand) for 7 days. After completion of drug treatments, will be used for MRI analysis and tissues will be collected for biochemical and histopathological study

Methods

1. MRI scanning

MR images of tissues were acquired using a high field, 1.5 T Siemens Magnetom (Siemens AG, Medizinische Technik, Germany). MRI protocol was determined using a modification of the method described by Grabill et al. (2003). Images were acquired using an 89-mm Helmholtz transmit RF coil and an 8×15-mm ellipsoidal receive surface RF coil, built to conform to the shape of the mouse skull so as to optimize signal-to-noise over the entire mouse brain. After positioning the mouse head in the magnet isocenter, global shimming was performed, and tri-pilot spin-echo scout images were obtained to aid slice positioning for the multi-slice T2 maps. T2 maps were obtained using a Carr, Purcell, Meiboom, Gill (CPMG) multi-echo spin-echo sequence with the following parameters: field of view (FOV)=2.56×2.56 cm2; matrix size=256×256; slice thickness=250 μm; NEX=1; repetition time (TR)=10 s; inter-

echo time (TE)=10 ms; number of echoes=8. The corresponding nominal resolution of each pixel was 100×100×250 μm2. Total scan acquisition time was on the order of 42 min. The typical signal-to-noise ratio (SNR) for this sequence was 56:1 (Grabill et al., 2003). All scans were reported at the time of acquisition by multiple operators, and a clinical report was generated for the referring physician.

To analyze the T2* values of brain and liver of β-thalassemic mice using Cardiovascular magnetic resonance (CMR) T2*, CMR techniques employing T2 measurements by the spin-echo (SE) sequence (or its variant) were useful in quantifying brain and liver iron (Anderson et al., 2001).

2. Measurement of tissues iron content

The levels of non-heme iron in the tissues were determined using a modification of the ferrozine method described by Foy et al. (1967). Tissue homogenates were prepared in high-purity water. Equal volumes of tissue homogenates and protein precipitation solution (1 N HCl and 10% trichloroacetic acid in high-purity water). Supernatant aliquots were mixed with chromogen solution and measurement of absorbance at 562.0 nm by spectrophotometry (Yatmark et al., 2014).

3. Histopathological studies

Tissues were dissected and preserved for routine histology by fixation in 4% paraformaldehyde, 5% sucrose and 150 mM PBS, pH 7.4. The fixed tissues were dehydrated and embedded in paraffin, sectioned to 5 μm thick. Serial sections were stained with Hematoxylin and Eosin staining method (H&E) for morphological changes and with Perls' Prussian blue

staining method for iron deposition by standard procedures (Hall et al. 2013). The tissue slides were examined by light microscopy on a Nikon ECLIPSE E200 (Tokyo, Japan).

Statistical analysis

Statistical analysis was performed with SPSS software version 19.0. The data were expressed as the means ± SD unless otherwise indicated. Data with a normal distribution are presented as mean ± SD. The comparisons were analyzed by one way analysis of variance (ANOVA) with Dunnett test as a post test. Pearson correlation as a measure of iron content and T2* MRI of a relationship between brain and liver. Statistical significance was considered when the p-value <0.05.

Results

Brain and liver iron content

Iron accumulation in the brain was observed in the brain of β-thalassemic mice 0.08±0.00 mg/g. Brain iron concentration increased in iron overloaded β-thalassemic mice 7.76±1.39 mg/g (Fig. 1). It was significantly increased when comparing with control group (P=0.001). Treatment with deferiprone was significantly reduced iron deposition in the brain 4.75±0.63 mg/g (P=0.021).

Naturally, β-thalassemic mice revealed a slight iron accumulation in the tissues even without iron loading in the liver 3.40±0.05 mg/g. Loading with iron dextran markedly significant increased iron content in β-thalassemic mice 17.92±2.44 mg/g (P<0.001). Treatment with deferiprone tended to reduce liver iron content in β-thalassemic mice 16.12±1.51 mg/g (Fig. 2) (P=0.307).

Figure 1: Brain iron content of β-thalassemic mice, iron overloaded, deferiprone. The errors bars refer to the standard deviation (SD)

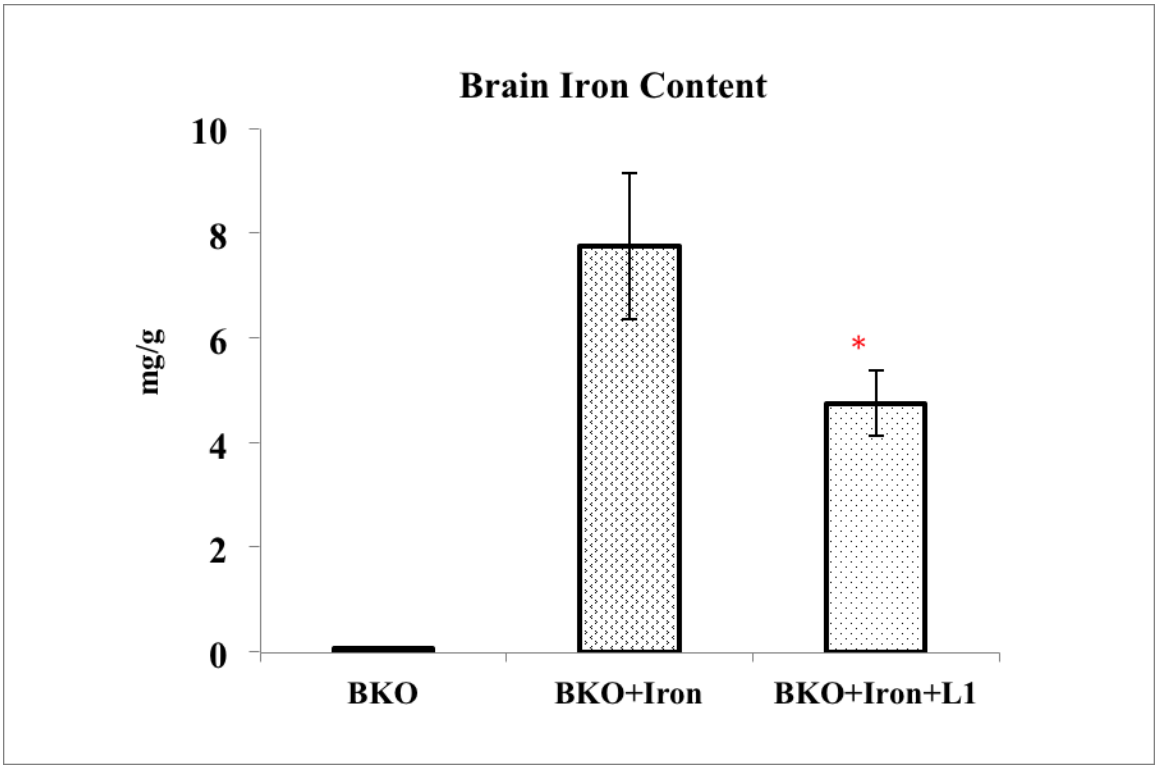

Figure 2: Brain iron content of β-thalassemic mice, iron overloaded, deferiprone. The errors bars refer to the standard deviation (SD)

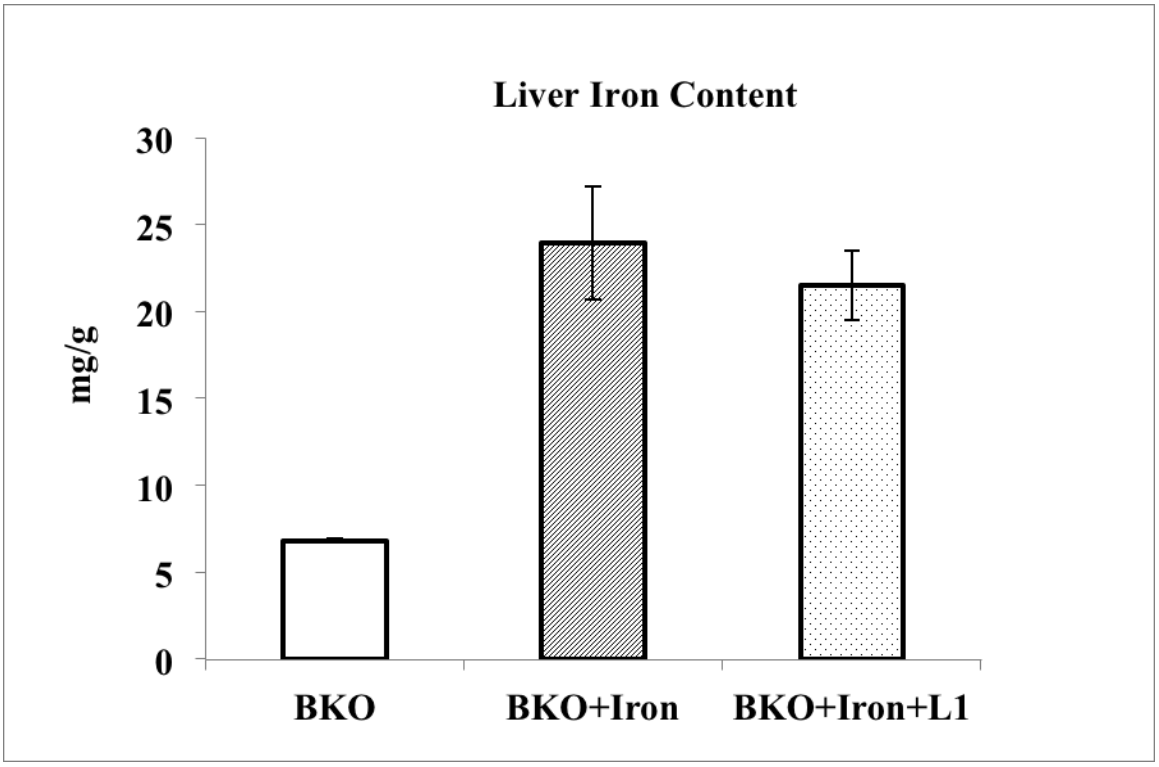

Brain and liver MRI: T2* values

T2* levels were calculated using the CMRtools/Thalassemia Tools. Calculated mean T2* value of each group are presented in Fig. 3 for the brain and Fig. 4 for the liver. The control brain T2* was 28.51±4.53 ms and the group of iron overload 9.80±0.94 ms. The iron overloaded group showed shorter T2* values, consistent with increased ferritin iron than control group. Brain T2* decreased with increasing iron deposition. The treatment of iron chelation was performed. The result demonstrated that deferiprone was significant decreased iron deposition in the brain. Brain T2* values was significant increased in the group of the treatment of deferiprone 17.87±3.85 ms (P=0.008).

The control liver T2* was 27.18±7.58 ms and the group of iron overload 5.22±2.21ms. The iron overloaded group showed shorter T2* values, consistent with increased ferritin iron than control group. Liver T2* decreased with increasing iron deposition. The treatment of iron chelation was performed. The result demonstrated that deferiprone was significant decreased iron deposition in the liver. Liver T2* values was significant increased in the group of the treatment of deferiprone 15.78±3.54ms (P=0.001).

Our results may useful to understand brain pathology in iron overload. Moreover, data could lead to earlier diagnosis, assist in following disease progression, and the benefits of iron chelation therapy.

Figure 3: Brain T2* values of β-thalassemic mice, iron overloaded, deferiprone. The errors bars refer to the standard deviation (SD)

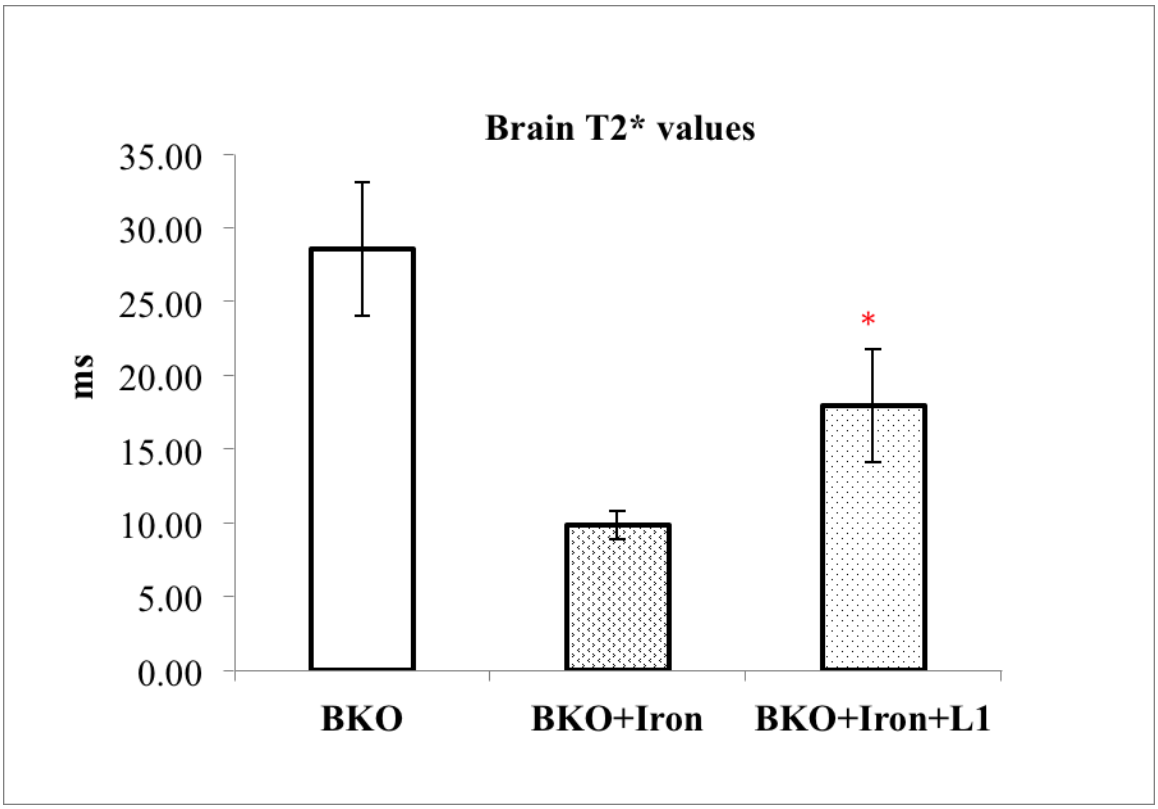

Figure 4: Brain iron content of β-thalassemic mice, iron overloaded, deferiprone. The errors bars refer to the standard deviation (SD).

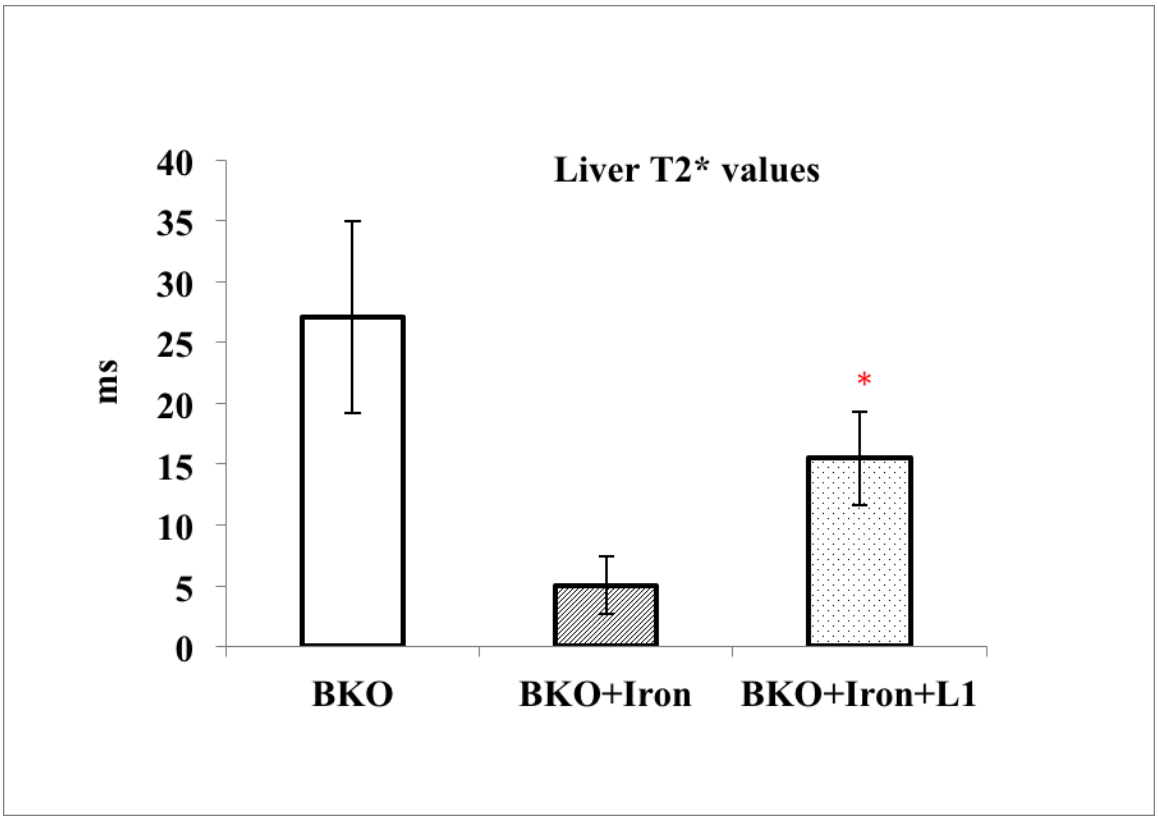

Quantitative MRI based histogram analyses

This study demonstrated MRI finding the brain of β-thalassemic mice. T2W showed hypointensity in region of interest. MRI images in regions. In the iron overload group, the histogram analyses of the 3 brain regions including cortex-cerebellar white matter, superior colliculus, and fimbria of hippocampus showed increase signal intensity and increase in the frequency of occurrence of pixels with shorter T2 values, consistent with increased ferritin iron.

The T2 histograms of the 3 brain regions including cortex-cerebellar white matter, superior colliculus, and fimbria of hippocampus in iron overloaded β-thalassemic mice group showed decrease when comparing with the control mice. This result demonstrated that the 3 regions of the brain of iron overloaded group were hypointensity than control mice, which related with the results that we found in the MRI finding.

The correlation of brain and liver

The correlation between iron content and T2* MRI as primary outcome, Pearson's correlation coefficient was calculated. Our results shown that negative correlation between brain iron content and T2* MRI brain ($R = -0.872$, $P < 0.001$) and also correlation between liver iron content and T2*MRI liver ($R = -0.797$, $P < 0.001$). Additionally, T2* MRI brain and T2* MRI liver shown positive correlation ($R = 0.849$, $P < 0.001$) and also brain iron content with liver iron content ($R = 0.877$, $P < 0.001$). The correlation of brain and liver as shown in Fig. 5-8.

Figure 5: Relationship between brain iron content and brain T2* values. Brain iron content strongly correlates with results of brain T2* value (R = -0.872, P< 0.001).

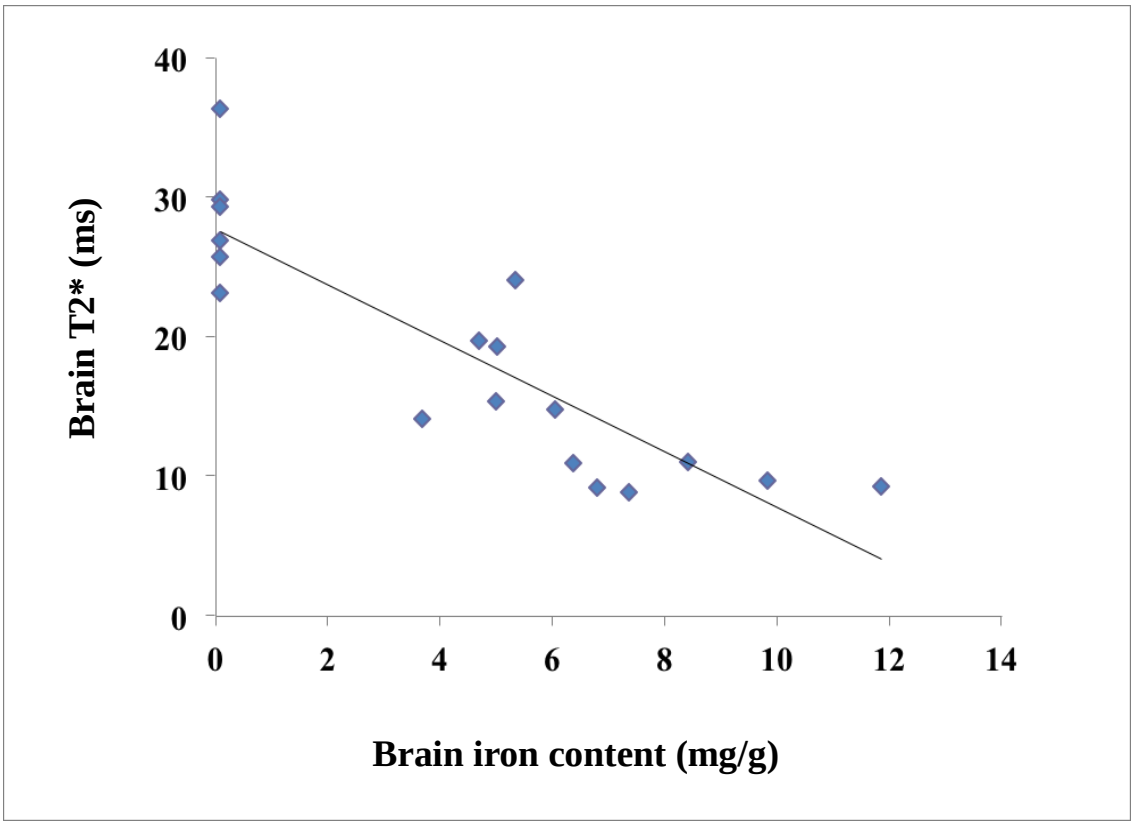

Figure 6: Relationship between liver iron content and liverT2* values. Liver iron content strongly correlates with results of liver T2* value (R = -0.797, P< 0.001).

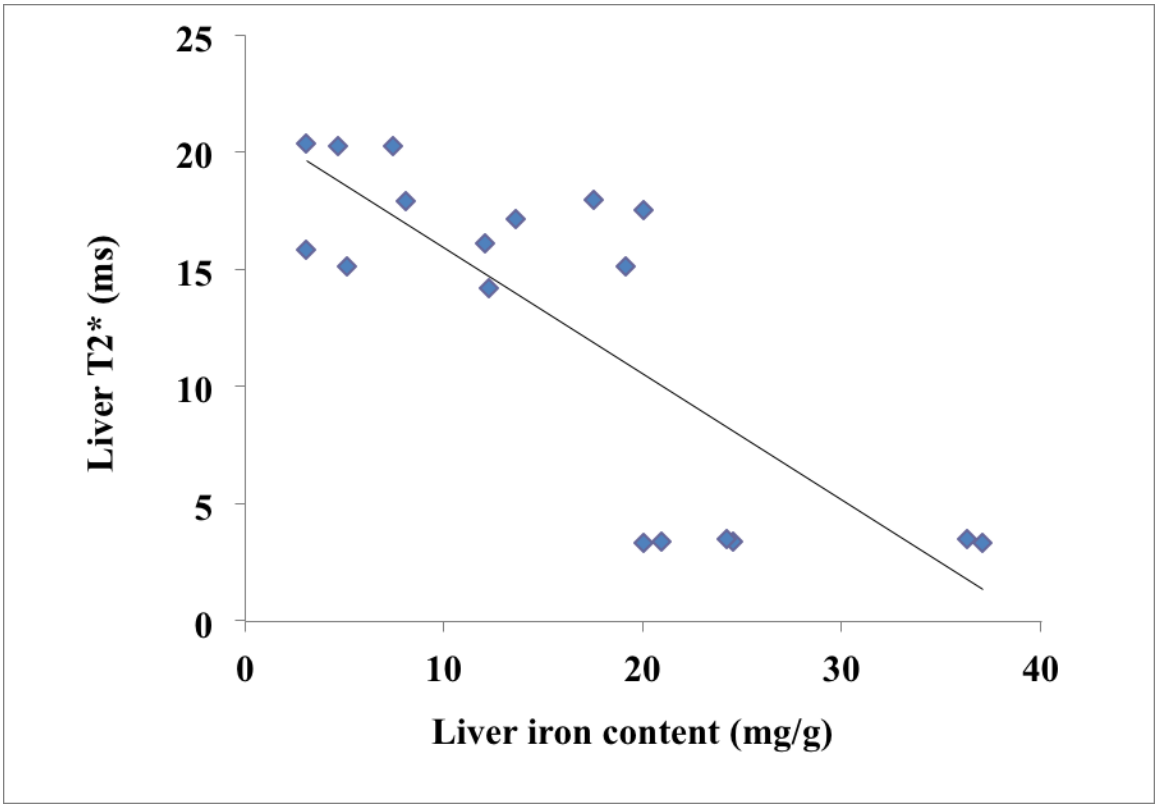

Figure 7: Relationship between brain T2* values and liver T2* values Brain T2* values strongly correlates with results of liver T2* values (R = 0.849, P< 0.001).

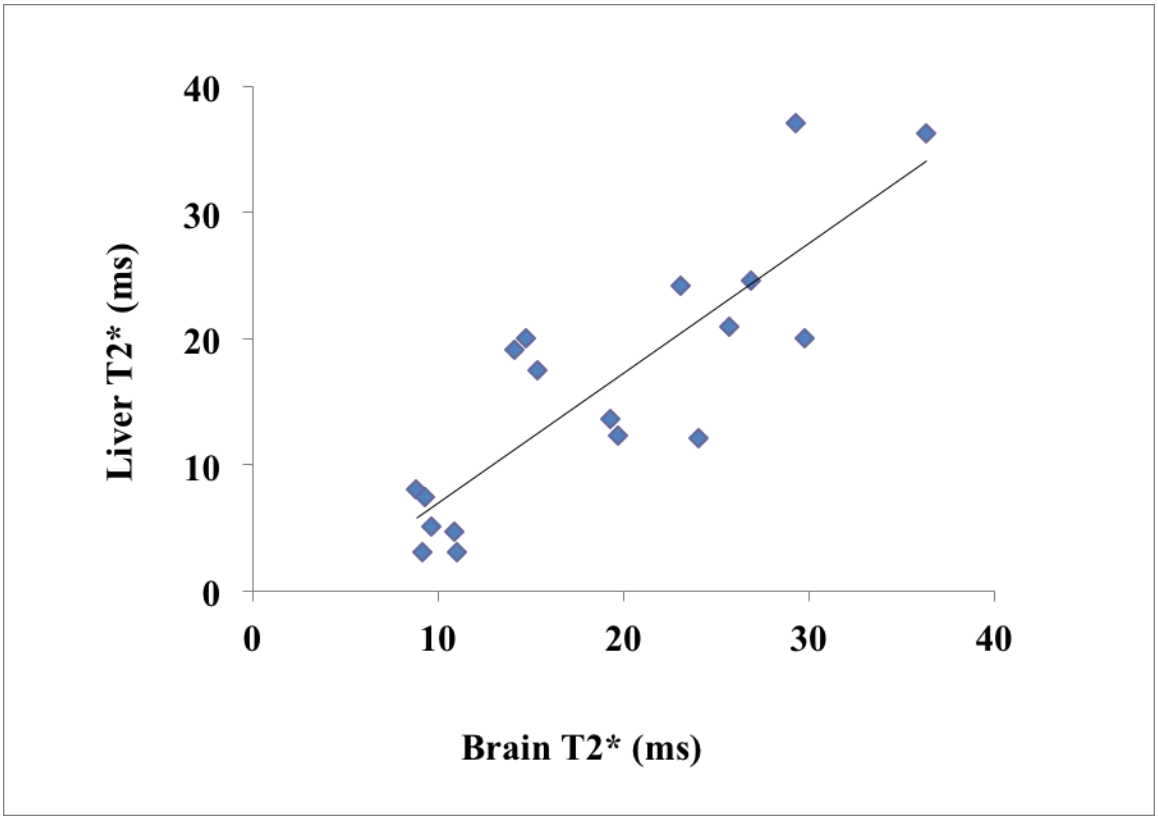

Figure 8: Relationship between brain iron content and liver iron content. Brain iron content strongly correlates with results of liver iron content (R = 0.877, P< 0.001).

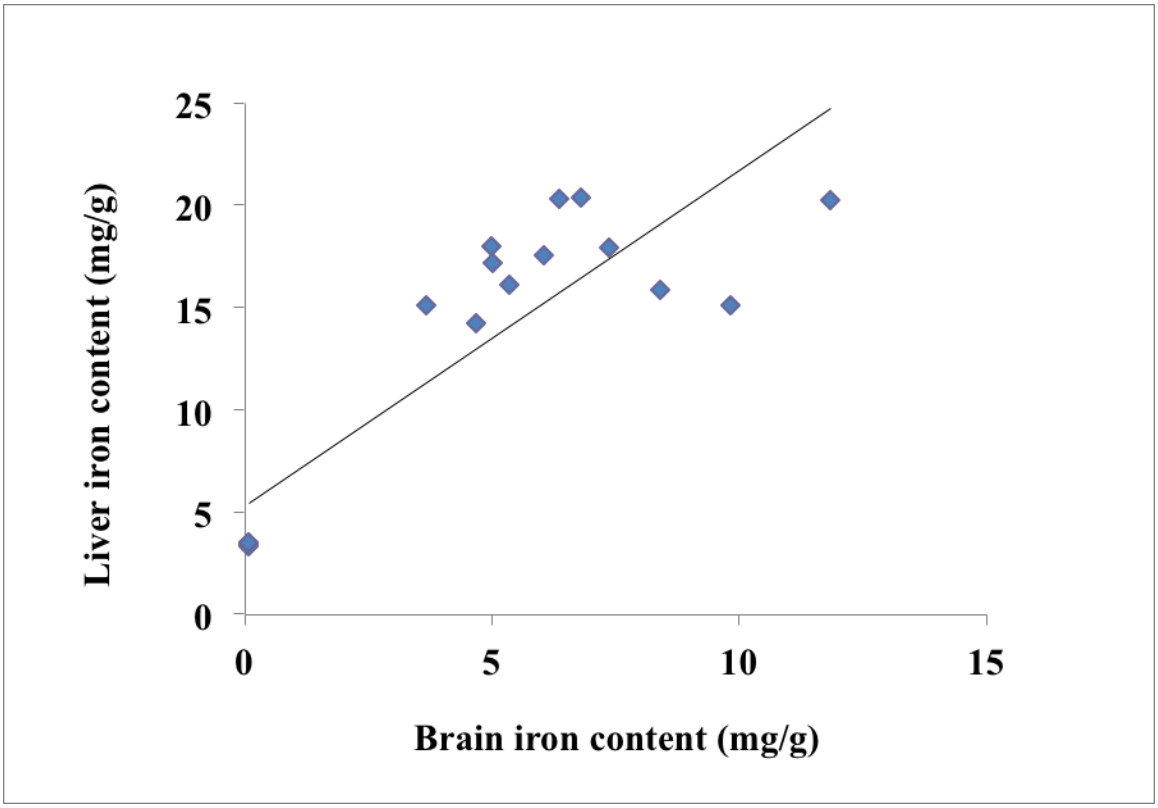

Brain and liver histopathology

Prussian blue staining

Figure 9 and Figure 10 show a representative image of the Prussian blue staining of the brain and liver of β-thalassemic mice, respectively. Spontaneous iron deposition was observed in the brain β-thalassemic mice, shown in microglia cell. After iron loading, iron was found in several area of brain including cerebral cortex, cerebellum, and choroid plexus. Treatment with deferiprone, found iron accumulation decreased in cerebral cortex and cerebellum.

In β-thalassemic mice, spontaneous iron deposition was observed in the Kupffer cells and hepatocytes. After iron loading, the iron was largely confined to clusters of phagocytic cells such as the Kupffer cells. Hemosiderin granules were observed in the cytoplasm of hepatocytes. Treatment with deferiprone decreased the size of the clusters of phagocytic cells.

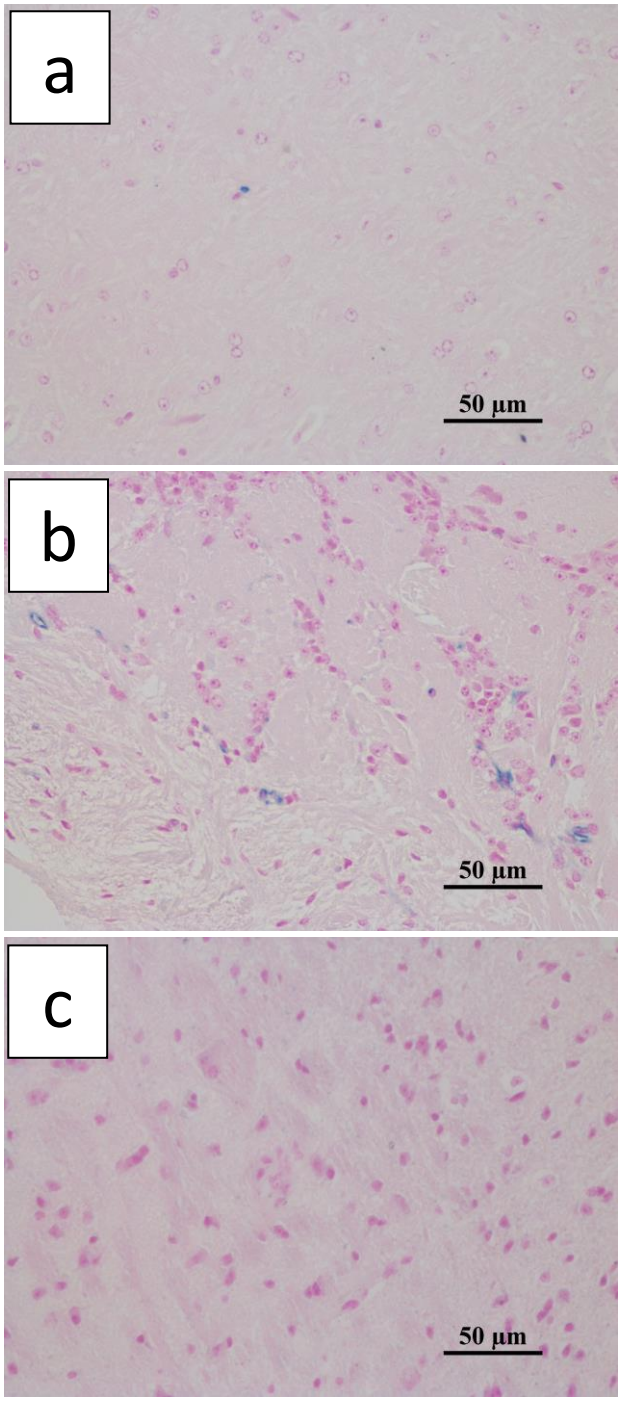

Figure 9: Perls' Prussian blue staining of brain of BKO mice. Control (a), iron overload (b) and iron-overloaded mice treated with deferiprone (c). The bar represents 50 mm, and the images were taken at 400x original magnification.

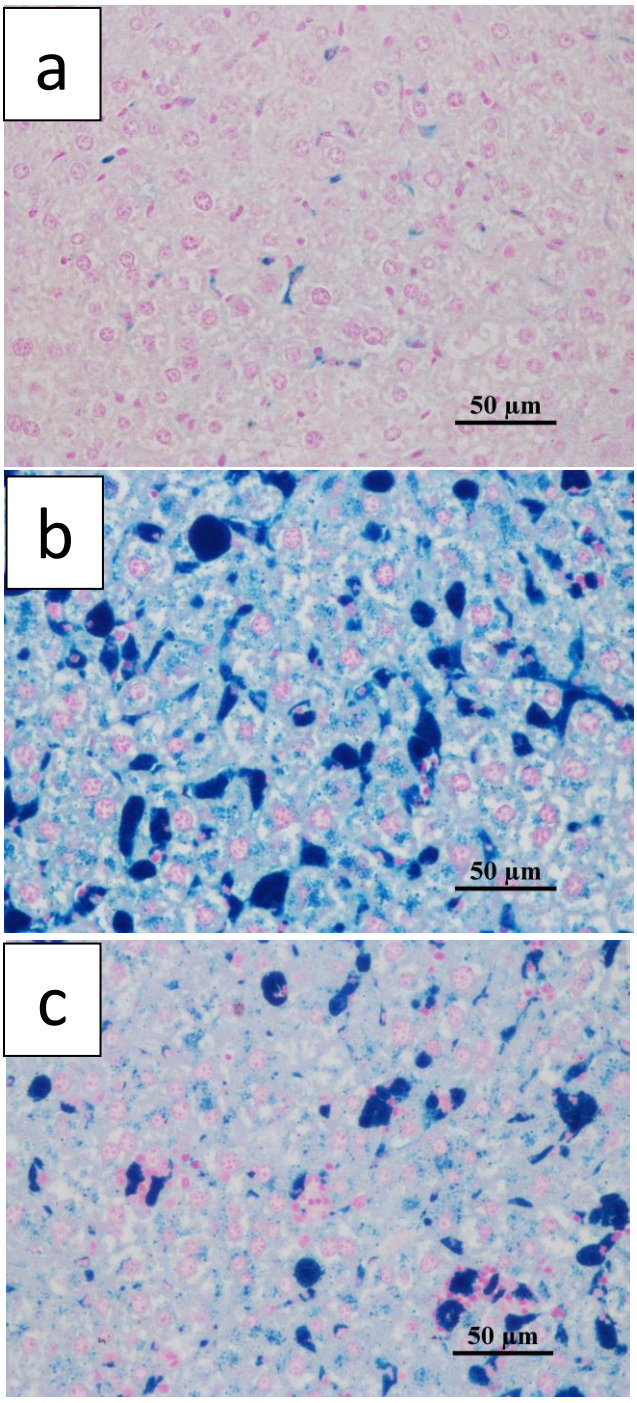

Figure 10: Perls' Prussian blue staining of liver of BKO mice. Control (a), iron overload (b) and iron-overloaded mice treated with deferiprone (c). The bar represents 50 mm, and the images were taken at 400x original magnification.

Hematoxylin and eosin staining

Hematoxylin and eosin (H&E) stained brain sections of β-thalassemic mice as shown in Fig.11. There was shown signs of hyperchromatic cells, vascular congestion and vaculated cells in the cerebral cortex, and cellular necrosis. Large cells which are mostly multipolar, neuronal swelling, chromatolysis and nuclear margination were observed (H&E×400). The iron-overloaded β-thalassemic mice, presence of clumps of brown pigment in microglia cell.

Signs of liver injury, including fatty liver and nuclear membrane degeneration, were observed in the β-thalassemic mice (data not shown). Changes in morphology were observed in the iron-overloaded β-thalassemic mice, including the presence of clumps of brown pigment in sinusoid-lining cells and swollen Kupffer cells and hepatocytes. A higher frequency of nuclear degeneration in the hepatocytes was observed in iron-overloaded mice. However, treatment with deferiprone decreased the size of the foci, and they became more ellipsoidal than spherical in shape.

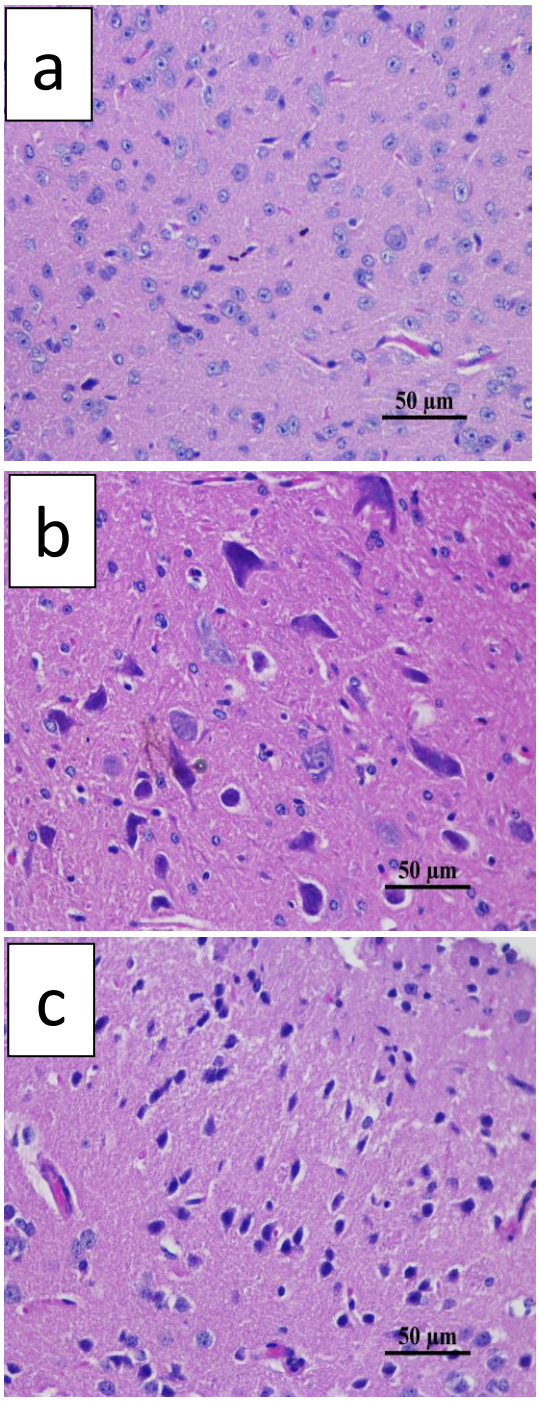

Figure 11: Hematoxylin and eosin staining of the brain of BKO mice. Control (a), iron overload (b) and iron-overloaded mice treated with deferiprone (c). The bar represents 50 mm, and the images were taken at 400x original magnification.

Conclusion and Discussion

In this study, we investigated and monitoring the utility of T2* for quantification of iron accumulation using MRI method in β-thalassemic mice. Additionally, the effect of iron chelator, deferiprone was examined in iron overloaded β-thalassemic mice model. Our results demonstrated that there was significant decreased iron accumulation in the brain in the treatment of deferiprone compared to iron overloaded β-thalassemic mice. In the brain, T2* values was significant decreased in the treatment of deferiprone, as same as results of liver. Although, liver iron content was not significant decreased in the treatment with deferiprone. However, it was tended to reduce liver iron content in β-thalassemic mice.

Previous studies shown that the MRI was a useful parameter to quantify hepatic iron concentration both in human (Alustiza et al., 2007; Ernst et al., 1999), and animal studies (Gandon et al., 2004; St Pierre et al., 2005). However, there is no validated sequence for the determination of brain iron concentration. In human, T2* MRI is the primary technique for identifying pathological iron overload in thalassemia patient (Pennell et al., 2013). T2 has also been shown to be a useful and reproducible measure of tissue iron in humans, however T2* remains the gold standard due to the substantial number of validation studies (He et al., 2006; 2008). The signal hypointensity was observed on routine clinical T2-weighted MRI sequences on a 1.5T scanner, although it was better localized with T2* weighted MRI. This results corresponded to the localization of increased iron on the tissue histology.

Iron has a critical role as a cofactor in many regulatory enzymes involved in cellular metabolic pathways, such as the electron transport chain in the mitochondria. It is particularly important in the CNS due to the high metabolic activity of the brain. Although brain iron content increases with age (Zecca et al., 2004), pathological accumulation of iron is postulated to be

pathogenic in several neurodegenerative disorders such as neurodegeneration with brain iron accumulation, Parkinson and Alzheimer disease (Rouault et al., 2006). Our study showed that iron was also increased in the brain using histological methods. Even though the motor cortex is known to have the highest concentration of iron in the human cerebral cortex, it is usually undetectable on histologic sections. This localization in the cortical grey differed from previous histologic studies of brain iron in individuals without neurological disorders in which intracellular iron accumulation in the cortex was mostly found in oligodendroglia (Connor et al., 1990).

It is uncertain what leads to the increased iron deposition in the motor cortex: misregulation of iron metabolism in motor neurons or microglia could cause disease, or microglia could accumulate iron as they scavenge debris that remains after neuronal degeneration. In the CNS, the iron transport protein transferrin is a component of Bunina bodies (Goodall et al., 2008), an intracytoplasmic inclusion in spinal motor neurons that is considered to be a pathological hallmark of neurodegeneration and iron accumulation in oligodendroglia were also seen in mutant mice with targeted deletions of iron regulatory protein-2 (Jeong et al., 2011). We could not identify iron accumulation within cortical or spinal motor neurons in β-thalassemic mice, which may indicate that if iron misregulation is the primary pathology, its origin is in non-neuronal cells. Of note, there was also no evidence of systemic iron overload in β-thalassemic mice. Activated microglial cells are a prominent component in both acute CNS injuries and chronic neurodegenerative disorders (Henkel et al., 2009). An important function of the microglia is phagocytosis of cellular debris after neuronal injury, and this has been suggested to provide a more favorable environment to facilitate the repair process (Neumann et al., 2009). Consistent with their role in removal of degenerated tissue, many microglial cells were seen in

the motor cortex and spinal cord where degenerating motor neurons and their axons are found. Iron and microglia are known to accumulate at the sites of neurodegeneration in Alzheimer and Parkinson disease (Ward et al., 2011). Microglial iron accumulation has been reported in the striatum of the transgenic mouse model of Huntington disease (Simmons et al., 2007). The association between regions with degenerating neurons and microglial iron accumulation may be related to microglia's role in the maintenance of brain iron homeostasis by scavenging excess iron and storing it in ferritin (Connor et al., 1994). We favor the interpretation that the intracellular iron in the microglial cells is derived from phagocytosis of degenerated neurons and glial cells.

Several different mechanisms have been proposed as the cause of neurodegeneration in thalassemia disease including oxidative stress and mitochondrial dysfunction (Sarki et al., 2017). Iron has been implicated in the pathogenesis of several neurodegenerative disorders due to its ability to generate cytotoxic reactive radicals that produce oxidative stress. However, a pathogenic role in thalassemia disease is unclear. Whether intracellular iron accumulation represents an upstream or downstream phenomenon in the disease process remains undetermined.

Further considerate of normal iron metabolism in neurons and glial cells is necessary to determine if unusual iron regulation contributes to pathology in thalassemia disease. The levels of serum ferritin was measured, it was significantly higher in iron-overloaded mice. A major function of ferritin is the storage of iron in an insoluble and non-toxic state (Carrondo, 2003). Large amounts of iron that are not stored within cells are, in general, considered to be the most potent potential toxin to cells. Several techniques have been developed that detect MR signal alterations derived mainly from the magnetic properties of hemosiderin, the major iron storage

compounds (Dusek et al., 2013). Longitudinal studies of a larger of thalassemic mice and controls are needed to determine whether the grading of hypointensity on T2-weighted MRI increases as degeneration progresses and whether it represents progressive iron accumulation.

In conclusion, we have demonstrated that T2* MRI can be used to detect iron accumulation in β-thalassemic mice. Our brain T2* values received from CMR software, in accordance with brain iron content, showed that was significantly increased iron accumulation in iron overloaded β-thalassemic mice. In addition, deferiprone treatment can be decreased brain iron accumulation. These MRI techniques may be useful for the detection of iron accumulation, and for monitoring iron levels in brain of β-thalassemic mouse models.

References

Altamura S, MU Muckenthaler.Iron toxicity in diseases of aging: Alzheimer's disease, Parkinson's disease and atherosclerosis.J Alzheimers Dis. 2009; 16(4):879-95.

Anderson LJ, Holden S, Davis B, et al. Cardiovascular T2-star (T2*) magnetic resonance for the early diagnosis of myocardial iron overload. Eur Heart J 2001; 22(23):2171–9.

Argyropoulou MI, Metafratzi Z, Kiortsis DN, Bitsis S, Tsatsoulis A, Efremidis S. T2 relaxation rate as an index of pituitary iron overload in patients with beta-thalassemia major. AJR Am J Roentgenol 2000; 175(6):1567–9.

Argyropoulou MI, Kiortsis DN, Astrakas L, Metafratzi Z, Chalissos N, Efremidis SC. Liver, bone marrow, pancreas and pituitary gland iron overload in young and adult thalassemic patients: a T2 relaxometry study. Eur Radiol 2007; 17(12):3025–30.

Blasco G, Puig J, Daunis-I-Estadella J, Molina X, Xifra G, Fernández-Aranda F, Pedraza S,

Ricart W, Portero-Otín M, Fernández-Real JM.Brain iron overload, insulin resistance, and cognitive performance in obese subjects: a preliminary MRI case-control study. Diabetes Care 2014; 37(11):3076-83.

Borgna-Pignatti C, Cappellini MD, Stefano DEP, et al. Survival and complications in thalassemia. Ann NY Acad Sci 2005; 1054:40–7.

Becerril-Ortega J, Bordji K, Fréret T, Rush T, Buisson A. Iron overload accelerates neuronal amyloid-b production and cognitive impairment in transgenic mice model of Alzheimer's disease. Neurobiology of Aging 2014;2288-2301.

Brass SD, Benedict RH, Weinstock-Guttman B, Munschauer F, Bakshi R. Cognitive impairment is associated with subcortical magnetic resonance imaging grey matter T2 hypointensity in multiple sclerosis. Mult Scler 2006;12:437-444.

Berg D, Youdim MB. Role of iron in neurodegenerative disorders. Top. Magn. Reson. Imaging 2006; 17, 5–17.

Brittenham GM, Farrell DE, Harris JW, Feldman ES, Danish EH, Muir WA, Tripp JH, Bellon EM. Magnetic-susceptibility measurement of human iron stores. N Engl J Med. 1982; 307(27):1671-5.

Brittenham GM, Badman DG. Noninvasive measurement of iron: report of an NIDDK workshop. Blood 2003; 101(1):15–9.

Bergeron C, Kovacs K.Pituitary siderosis. A histologic, immunocytologic, and ultrastructural study. Am J Pathol. 1978; 93(2):295-309.

Boddaert N, Le Quan Sang KH, Rötig A, Leroy-Willig A, Gallet S, Brunelle F, Sidi D, Thalabard JC, Munnich A, Cabantchik ZI.Selective iron chelation in Friedreich ataxia: biologic and clinical implications. Blood. 2007; 110(1):401-8.

Brasch RC, Wesbey GE, Gooding CA, Koerper MA.Magnetic resonance imaging of transfusional hemosiderosis complicating thalassemia major. Radiology. 1984; 150(3):767-71.

Bothwell TH. Overview and mechanisms of iron regulation. Nutr Rev. 1995; 53(9):237-45.

Bartzokis G, Mintz J, Marx P, Osborn D, Gutkind D, Chiang F, Phelan CK, Marder SR. Reliability of in vivo volume measures of hippocampus and other brain structures using MRI. Magn Reson Imaging. 1993; 11(7):993-1006.

Bartzokis G, Sultzer D, Cummings J, Holt LE, Hance DB, Henderson VW, Mintz J. In vivo evaluation of brain iron in Alzheimer disease using magnetic resonance imaging. Arch Gen Psychiatry. 2000; 57(1):47-53.

Carrondo MA.Ferritins, iron uptake and storage from the bacterioferritin viewpoint. EMBO J. 2003 May 1;22(9):1959-68. Review

Carpenter JP, He T, Kirk P, Roughton M, Anderson LJ, de Noronha SV, Sheppard MN, Porter JB, Walker JM, Wood JC, Galanello R, Forni G, Catani G, Matta G, Fucharoen S, et al. On T2* magnetic resonance and cardiac iron. Circulation. 2011; 123(14):1519-28.

Crichton RR. Inorganic Biochemistry or Iron Metabolism from Molecular Mechanisms to Clinical Consequences. Chichester: John Wiley & Sons, Ltd (2009).

Christoforidis A, Haritandi A, Tsitouridis I, Tsatra I, Tsantali H, Karyda S, Dimitriadis AS, Athanassiou-Metaxa M. Correlative study of iron accumulation in liver, myocardium, and pituitary assessed with MRI in young thalassemic patients. J Pediatr Hematol Oncol. 2006; 28(5):311-5.

Chinnery PF, Crompton DE, Birchall D, Jackson MJ, Coulthard A, Lombès A, Quinn N, Wills

A, Fletcher N, Mottershead JP, Cooper P, Kellett M, Bates D, Burn J. Clinical features and natural history of neuroferritinopathy caused by the FTL1 460InsA mutation. Brain. 2007; 130:110-9.

Connor JR, Menzies SL, St Martin SM, Mufson EJ.Cellular distribution of transferrin, ferritin, and iron in normal and aged human brains. J Neurosci Res. 1990; 27(4):595-611.

Connor JR, Boeshore KL, Benkovic SA, Menzies SL. Isoforms of ferritin have a specific cellular distribution in the brain. J Neurosci Res. 1994;37:461–465.

Deoni SC, Catani M. Visualization of the deep cerebellar nuclei using quantitative T1 and rho magnetic resonance imaging at 3 Tesla. Neuroimage. 2007; 37(4):1260-6.

Dringen R, Bishop GM, Koeppe M, Dang TN, Robinson SR. The pivotal role of astrocytes in the metabolism of iron in the brain. Neurochem Res. 2007; 32(11):1884-90.

Dusek P, Schneider SA. Neurodegeneration with brain iron accumulation Curr Opin Neurol. 2012; 25(4):499-506.

Dixon ML, Christoff K.The decision to engage cognitive control is driven by expected reward-value: neural and behavioral evidence. PLoS One. 2012; 7(12):e51637.

Duce JA, Bush AI. Biological metals and Alzheimer's disease: implications for therapeutics and diagnostics. Prog. Neurobiol. 2010; 92:1–18.

Duce JA, Tsatsanis A, Cater MA, James SA, Robb E, Wikhe K, et al. Iron-export ferroxidase activity of beta-amyloid precursor protein is inhibited by zinc in Alzheimer's disease. Cell 2010); 142 857–867.

Foy AL, Williams HL, Cortell S, Conrad ME: A modified procedure for the determination of non-heme iron in tissue. Anal Biochem 1967; 18:559-63.

Fischer H, Gottschlich R, Seelig A. Blood-brain barrier permeation: molecular parameters governing passive diffusion. J Membr Biol. 1998; 165(3):201-11.

Fragasso A, Ciancio A, Mannarella C, Gaudiano C, Scarciolla O, Ottonello C, Francone M, Nardella M, Peluso A, Melpignano A, Veglio MR, Quarta G, Turchetti C. Myocardial iron overload assessed by magnetic resonance imaging (MRI)T2* in multi-transfused patients with thalassemia and acquired anemias. Eur J Intern Med. 2011; 22(1):62-5.

Gerlach M, Ben-Shachar D, Riederer P, Youdim MB. Altered brain metabolism of iron as a cause of neurodegenerative diseases? J Neurochem. 1994; 63(3):793-807.

Grabill C, Silva AC, Smith SS, Koretsky AP, Rouaulta TA. MRI detection of ferritin iron overload and associated neuronal pathology in iron regulatory protein-2 knockout mice. Brain Research 2003; 971:95–106.

Goodall EF, Haque MS, Morrison KE. Increased serum ferritin levels in amyotrophic lateral sclerosis (ALS) patients. J Neurol. 2008;255:1652–1656

Haacke EM, Cheng NY, House MJ, Liu Q, Neelavalli J, Ogg RJ, et al. Imaging iron stores in the brain using magnetic resonance imaging. Magn. Reson. Imaging 2005; 23:1–25.

Hall AP, Davies W, Stamp K, Clamp I, Bigley A.Comparison of computerized image analysis with traditional semiquantitative scoring of Perls' Prussian Blue stained hepatic iron deposition. Toxicol Pathol. 2013; 41(7):992-1000.

Hocq A, Brouette N, Saussez S, Luhmer M, Gillis P, Gossuin Y. Variable-field relaxometry of iron-containing human tissues: a preliminary study. Contrast Media Mol Imaging 2009; 4(4):157-64.

Huang X, Atwood CS, Moir RD, Hartshorn MA, Tanzi RE, Bush AI. Trace metal contamination initiates the apparent auto-aggregation, amyloidosis, and oligomerization of Alzheimer's Abeta peptides. J. Biol. Inorg. Chem 2004; 9 954–960.

Jamsai D, Zaibak F, Khongnium W, Vadolas J, Voullaire L, Fowler KJ, Gazeas S, Fucharoen S, Williamson R, Ioannou PA: A humanized mouse model for a common beta-thalassemia mutation. Genomics 2005; 85:453-61.

Jensen CE, Tuck SM, Old J, et al. Incidence of endocrine complications and clinical disease severity related to genotype analysis and iron overload in patients with beta-thalassaemia. Eur J Haematol 1997; 59(2):76– 81.

Jensen PD, Jensen FT, Christensen T, Heickendorff L, Jensen LG, Ellegaard J. Indirect evidence for the potential ability of magnetic resonance imaging to evaluate the myocardial iron content in patients with transfusional iron overload. MAGMA 2001; 12:153–66.

Jeong SY, Crooks DR, Wilson-Ollivierre H, Ghosh MC, Sougrat R, et al. Iron insufficiency compromises motor neurons and their mitochondrial function in Irp2-null mice. PLoS One. 2011;6:e25404.

Ke Y, Ming Qian Z. Iron misregulation in the brain: a primary cause of neurodegenerative disorders. Lancet Neurol. 2003; 2(4):246-53.

Ke Y, Qian ZM. Brain iron metabolism: neurobiology and neurochemistry. Prog. Neurobiol. 2007; 83 149–173.

Kirk P, Roughton M, Porter JB, Walker JM, Tanner MA, Patel J, et al. Cardiac T2* magnetic resonance for prediction of cardiac complications in thalassemia major. Circulation 2009; 120:1961–8.

Khalil M, Teunissen C, Langkammer C. Iron and neurodegeneration in multiple sclerosis. Mult Scler Int. 2011; 2011:1-6.

Lee DW, Andersen JK. Role of HIF-1 in iron regulation: potential therapeutic strategy for neurodegenerative disorders. Curr Mol Med. 2006; 6(8):883-93.

Leitner DF, Connor JR. Functional roles of transferrin in the brain. Biochim Biophys Acta. 2012; 1820(3):393-402.

Langkammer C, Krebs N, Goessler W, Scheurer E, Ebner F, Yen K, Fazekas F, Ropele S. Quantitative MR imaging of brain iron: a postmortem validation study. Radiology 2010; 257(2):455-62.

Modell B, Khan M, Darlison M. Survival in beta-thalassaemia major in the UK: data from the UK Thalassaemia Register. Lancet 2000; 355(9220):2051-2.

Metafratzi Z, Argyropoulou MI, Kiortsis DN, Tsampoulas C, Chaliassos N, Efremidis SC. T2 relaxation rate of basal ganglia and cortex in patients with beta-thalassaemia major. Br J Radiol. 2001; 74(881):407-10.

Moos T, Rosengren Nielsen T, Skjørringe T, Morgan EH. Iron trafficking inside the brain. J Neurochem. 2007; 103(5):1730-40.

Madsen E, Gitlin JD. Copper and iron disorders of the brain. Annu Rev Neurosci 2007;30:317-37.

Noetzli LJ, Carson SM, Nord AS, Coates TD, Wood JC. Longitudinal analysis of heart and liver iron in thalassemia major. Blood 2008; 112(7):2973–8.

Noetzli LJ, Papudesi J, Coates TD, Wood JC. Pancreatic iron loading predicts cardiac iron loading in thalassemia major. Blood 2009; 114(19):4021–6.

Noetzli, L. J.,Mittelman, S. D., Watanabe, R. M.,etal. Pancreatic iron and glucose dysregulation in thalassemia major. Am J Hematol. 2012; 87:155–160.

Neumann H, Kotter MR, Franklin RJ. Debris clearance by microglia: an essential link between degeneration and regeneration. Brain. 2009;132:288–295.

Ott M, Stouffer C, Foote J, Foster A .Roux-en-Y gastric bypass: a novel approach to the treatment of hemochromatosis? Am J Hematol. 2007; 82(11):1033.

Olson LJ, Edwards WD, McCall JT, Ilstrup DM, Gersh BJ. Cardiac iron deposition in idiopathic hemochromatosis: histologic and analytic assessment of 14 hearts from autopsy. J Am Coll Cardiol. 1987; 10(6):1239-43.

Oerter KE, Kamp GA, Munson PJ, Nienhuis AW, Cassorla FG, Manasco PK. Multiple hormone deficiencies in children with hemochromatosis. J Clin Endocrinol Metab. 1993; 76(2):357-61.

Pennell DJ, Porter JB, Cappellini MD, El-Beshlawy A, Chan LL, Aydinok Y, et al. Efficacy of deferasirox in reducing and preventing cardiac iron overload in β- thalassemia. Blood 2010; 115:2364–71.

Qian ZM, Shen X. Brain iron transport and neurodegeneration. Trends Mol Med. 2001; 7(3):103-8.

Schipper HM. Heme oxygenase-1: transducer of pathological brain iron sequestration under oxidative stress. Ann NY Acad Sci 2004; 1012, 84-93.

Simmons DA, Casale M, Alcon B, Pham N, Narayan N, et al. Ferritin accumulation in dystrophic microglia is an early event in the development of Huntington's disease. Glia. 2007;55:1074–1084.

Rouault TA. Iron metabolism in the CNS: implications for neurodegenerative diseases. Nat. Rev. Neurosci 2013; 14:551–564.

Mounsey RB and Teismann P. Chelators in the Treatment of Iron Accumulation in Parkinson's Disease. Int J Cell Biol. 2012; 2012:1-12

Shaki F, Shayeste Y, Karami M, Akbari E, Rezaei M, Ataee R.The effect of epicatechin on oxidative stress and mitochondrial damage induced by homocycteine using isolated rat hippocampus mitochondria.Res Pharm Sci. 2017 Apr;12(2):119-127

Stankiewicz J, Panter SS, Neema M, Arora A, Batt CE, Bakshi R. Iron in chronic brain disorders:imaging and neurotherapeutic implications. Neurotherapeutics. 2007;4(3):371-86.

Schenck JF, Zimmerman EA. High-field magnetic resonance imaging of brain iron: birth of a biomarker? NMR Biomed. 2004; 17(7):433-45.

Srichairatanakool, S., Pangjit, K., Phisalaphong, C., Fucharoen, S. Evaluation of a novel oral iron chelator1-(N-acethyl-6-aminohexyl)-3-hydroxypyridin-4-one (CM1) for treatment of iron overload in mice. Adv Biosci Biotechnol 2013; 4:153-163.

Thomas LO, Boyko OB, Anthony DC, Burger PC. MR detection of brain iron. AJNR Am J Neuroradiol. 1993; 14(5):1043-8.

Utter AA, Basso MA. The basal ganglia: an overview of circuits and function. Neurosci Biobehav Rev. 2008; 32(3):333-42.

Vogiatzi MG, Macklin EA, Trachtenberg FL, Fung EB, Cheung AM, Vichinsky E, Olivieri N, Kirby M, et al. Differences in the prevalence of growth, endocrine and vitamin D abnormalities among the various thalassaemia syndromes in North America. Br J Haematol. 2009; 146(5):546-56.

Ward RJ, Crichton RR, Taylor DL, Della Corte L, Srai SK, et al. Iron and the immune system. J Neural Transm. 2011;118:315–328.

Wood JC, Enriquez C, Ghugre N, et al. MRI R2 and R2* mapping accurately estimates hepatic iron concentration in transfusion-dependent thalassemia and sickle cell disease patients. Blood 2005; 106(4):1460–5.

Wood JC. Magnetic resonance imaging measurement of iron overload. Curr Opin Hematol 2007; 14(3):183–90.

Wood JC, Ghugre N. Magnetic resonance imaging assessment of excess iron in thalassemia, sickle cell disease and other iron overload diseases. Hemoglobin. 2008; 32(1-2):85-96.

Wood JC, Noetzli L. Cardiovascular MRI in thalassemia major. Ann N Y Acad Sci. 2010; 1202:173-9.

Yatmark P, Morales NP, Chaisri U, Wichaiyo S, Hemstapat W, Srichairatanakool S, Svasti S, Fucharoen S: Iron distribution and histopathological characterization of the liver and heart of β-thalassemic mice with parenteral iron overload: effect of deferoxamine and deferiprone. Exp Toxicol Pathol 2014;66:333-43.

Yatmark P, Morales NP, Chaisri U, Wichaiyo S, Hemstapat W, Srichairatanakool S, Svasti S, Fucharoen S: Effects of iron chelators on pulmonary iron overload and oxidative stress in β-thalassemic mice. Pharmacology. In Press, 2015.

Yang B, Kirby S, Lewis J, Detloff PJ, Maeda N, Smithies OA. A mouse model for β0-thalassemia.Proc Natl Acad Sci1995; 92,11608-11612.

Zecca L, Youdim MB, Riederer P, Connor JR, Crichton RR. Iron, brain ageing and neurodegenerative disorders. Nat. Rev. Neurosci 2004; 5:863–873.

Appendix

Expected benefits

The results of this study will be provided a valuable knowledge in brain iron deposition in β-thalassemic mice that could applied for β-thalassemia patients. This model can be established to further evaluate the efficacy of iron chelators in clinical trials of thalassemia patients and other diseases. Moreover, measurement of brain iron deposition by MRI is a non-invasive direct method that has been developed for detecting and quantifying iron levels and might be reduce the risk of future neurodegenerative disease in thalassemia patients. Finally, the results from this study are expected to be published in appropriate peer-reviewed journals.

Output (Acknowledge the Thailand Research Fund)

8.1 International Journal Publication

Waiting for publication

8.2 Research Utilization and Application

N/A

8.3 Others e.g. national journal publication, proceeding, international conference, book chapter, patent

1. **Abstract**: Yatmark et al., Effect of deferiprone on brain iron distribution of β-thalassemic mice using Magnetic Resonance Imaging (MRI). The 17th TRF-OHEC Annual Congress 2018 (TOAC 2018), 10-12 Jan 2018, Petchburi, Thailand
2. **Proceeding**: Yatmark et al., Monitoring Hepatic Iron content in iron overloaded β-thalassemic mice using Magnetic Resonance Imaging. The 40th Pharmacological and Therapeutic Sociaty of Thailand meeting, 26-28 April 2018, Bangkok, Thailand

Effect of deferiprone on brain iron distribution of β-thalassemic mice using Magnetic Resonance Imaging (MRI)

Yatmark, P.[1*], Huaijantug, S.[2], Teerapan, W.[3], Svasti, S. [4],
Fucharoen, S. [5], Morales, NP.[6]

[1]*Department of Pre-clinic and Applied animal science, Faculty of Veterinary Science, Mahidol University, Nakorn Pathom, Thailand.*
[2]*Department of Clinical Sciences and Public Health, Faculty of Veterinary Science, Mahidol University, Nakorn Pathom, Thailand.*
[3]*Department of Companion Animals Clinical Sciences, Faculty of Veterinary medicine, Kasetsart University, Bangkok, Thailand.*
[4,5]*Institute of Molecular Biosciences, Mahidol University, Nakorn Pathom, Thailand.*
[6]*Department of Phamacology, Faculty of Science, Mahidol University, Bangkok, Thailand.*

Abstract

Brain iron overload is a chronic and slow progression that plays an important role in the pathogenesis of neurodegenerative disorders. Magnetic resonance imaging (MRI) is a useful non-invasive tool for determining liver iron content, but not proven to be adequate for evaluating brain iron overload. We evaluated the usefulness of MRI-derived parameters to determine brain iron concentration in β-thalassemic mice and the effects of membrane permeable iron chelator, deferiprone. Sixteen β-thalassemic mice underwent 1.5 T MRI of the brain that included a multiecho T2*-weighted sequence. Brain T2* values ranging from 28-31 ms for thalassemic mice. For the iron overloaded thalassemic mice, brain T2* values decreased to 8-12 ms, with correlated with iron overload status of the animals. In addition, brain T2* values increased in the group of the treatment of deferiprone ranging from 18-24 ms. Our results may useful to understand brain pathology in iron overload. Moreover, data could lead to earlier diagnosis, assist in following disease progression, and the benefits of iron chelation therapy.

Keywords: brain, iron, deferiprone, MRI

[*]Corresponding author.

Tel.: 02-4415242 ext. 1534; Fax: 02-4410937

E-mail: paranee.yat@mahidol.ac.th

Effect of deferiprone on brain iron distribution of β-thalassemic mice using MRI

Yatmark, P.[1*], Hunsjantug, S.[2], Teerapan, W.[3], Svasti, S.[4], Fucharoen, S.[4],Morales, NP.[5]

[1]Department of Pre-clinic and Applied animal science, Faculty of Veterinary Science, Mahidol University, Nakorn Pathom, Thailand.
[2]Department of Clinical Sciences and Public Health, Faculty of Veterinary Science, Mahidol University, Nakorn Pathom, Thailand.
[3]Department of Companion Animals Clinical Science, Faculty of Veterinary medicine, Kasetsart University, Bangkok, Thailand.
[4]Thalassemia Research Center, Institute of Molecular Biosciences, Mahidol University, Salaya Campus, Nakhon Pathom, Thailand.
[5]Department of Pharmacology, Faculty of Science, Mahidol University, Bangkok, Thailand.

Email: parunee.yat@mahidol.edu*

Introduction

Brain iron overload is a chronic and slow progression that is an initial cause of neuronal death and brain dysfunction. Iron accumulates only occurred in some specific regions of the brain of patients with neurodegenerative disorders. Our previous study has been established an animal model with iron overload in β-thalassemic mice which mimics the characteristics of iron overload in thalassemia. This model offers for physiological, histopathological studies and the assessment of the effects of pharmacological treatments in thalassemia without the limitations of research in human patients. In this model, brain iron accumulation was also observed.

Objectives

To optimize brain MRI protocols for studing the distribution of iron in the brain of iron overloaded β-thalassemic mice.

Materials and methods

Animal

Male and female heterozygous β-globin knockout mice (*hbb*th3/+*, BKO) 7 weeks of age and weighing 17-25 g were obtained from the Thalassemia Research Center, Institute of Science and Technology for Research and Development, Mahidol University, Thailand.

Group A: BKO mice :normal saline (0.9 %NaCl) (n=6)
Group B: BKO mice :iron dextran (20 mg/kg/day) (n=6)
Group C: BKO mice :iron dextran (20 mg/kg/day) + L1 (n=6)

MRI SCAN

Inject xylazine 25 mg/kg ip.

Scanning by 1.5 T Siemens Magnetom (Siemens AG, MedizinischeTechnik, Germany)

T2-weighted images

Quantitative T2* value by CMR2 software

Statistical analysis was performed with SPSS software version 19.0

Results

This study demonstrated the markedly increased brain iron content in BKO mice after loading with iron dextran. Treatment with deferiprone significantly reduced iron deposition in the brain of BKO mice. T2-Weighted image showed hypointensity in region of interest in iron overloaded mice. In the iron overload group, T2* values was decreased to 9.86±0.94 ms (mean±SD), corresponding with increased ferritin iron. The histogram analyses of cortex-cerebellar white matter showed increase signal intensity and increase in the frequency of occurrence of pixels with shorter T2*values. Treatment of an iron chelation, deferiprone, T2* value was statistically significant difference from the iron overloaded group.

Figure 1: Brain iron concentration in the normal, iron overloaded, and iron chelation (deferiprone) group of β-thalassemic mice

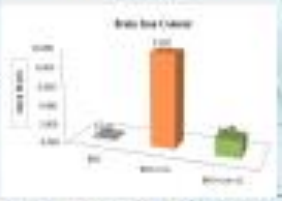

Figure 2: Brain T2* values in the normal, iron overloaded, and iron chelation(deferiprone) group of β-thalassemic mice

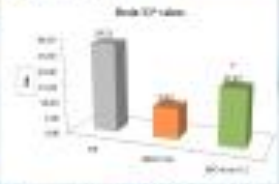

Figure 3: T2-weighted images in the normal, iron overloaded, and iron chelation (deferiprone) group of β-thalassemic mice

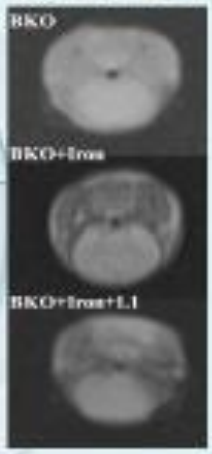

Figure 4: Region of interest selection. Green color mark areas identify the anatomical regions that were analyzed. T2 histogram were extracted from all pixels in each ROI and compared between the iron overloaded and control group of β-thalassemic mice

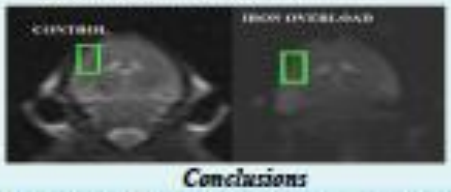

Conclusions

In conclusion, MRI echo sequence allowed a good estimation of iron overload in brain of β-thalassemia mice. The results demonstrated that brain T2* values were decreased to 9.86±0.94 ms for the iron overloaded thalassemic mice and correlated with iron overload status of the animals. In addition, brain T2* values increased in the group of the treatment of deferiprone, 17.87±3.85 ms. This MRI approach improved the physiopathological understanding of iron overload diseases and provided practical help for the follow-up of iron depletive treatment.

Acknowledgments

This study is supported by a grant from The Thailand Research Fund (MRG5980089). Deferiprone was kindly provided by The Government Pharmaceutical Organization, Bangkok, Thailand. The authors thank The Faculty of Veterinary Science, Mahidol University.

A15 Monitoring Hepatic Iron Content in Iron Overloaded β-Thalassemic Mice by Magnetic Resonance Imaging

Paranee Yatmark[1,*], Somkiat Huaijantug[2], Wanida Jesdachest[3], Tararat Bunvanno[3], Kamonwat Surareuangchai[3], Wuttiwong Teerapan[4], Saovaros Svasti[5], Suthat Fucharoen[5], Noppawan Phumala Morales[6]

[1]Department of Pre-clinic and Applied animal science, Faculty of Veterinary Science, Mahidol University, Nakorn Pathom 73170, Thailand
[2]Department of Clinical Sciences and Public Health, Faculty of Veterinary Science, Mahidol University, Nakorn Pathom 73170, Thailand
[3]Faculty of Veterinary Science, Mahidol University, Nakorn Pathom 73170, Thailand
[4]Department of Companion Animals Clinical Sciences, Faculty of Veterinary Medicine, Kasetsart University, Bangkok 10900, Thailand
[5]Institute of Molecular Biosciences, Mahidol University, Nakorn Pathom 73170, Thailand
[6]Department of Phamacology, Faculty of Science, Mahidol University, Bangkok 10400, Thailand
*E-mail: paranee.yat@mahidol.edu.

Abstract

Increasing of hepatocellular carcinoma in patients with β-thalassemia has been recognized in the past few years. Iron overload is a major cause of this advance complication, therefore monitoring of hepatic iron is necessary for early diagnosis and evaluation of iron chelation therapy. Magnetic resonance imaging (MRI) is known as a useful non-invasive tool for monitoring hepatic iron overload in β-thalassemia patients. However, this technique is limit to a small animal model. This study, MRI technique using T2*value was developed to study hepatic iron content and to monitor the effect of an iron chelator, deferiprone in β-thalassemic mice. Eighteen β-thalassemic mice underwent 1.5 T MRI of the liver and iron level was quantified using T2* value with cardiovascular magnetic resonance (CMR) software. The results showed that the liver T2* values of β-thalassemic mice was 18-37 ms. The values decreased to 3-8 ms in corresponding with increased hepatic iron content (15-20 mg/g liver) in iron loaded β-thalassemic mice (r=-0.797, p=0.001). Iron chelation with deferiprone (80 mg/g body weight) for 7 days, significantly increased liver T2* value to 11-21 ms. Our results demonstrated that the developed MRI technique using T2* CMR sequence was simple and applicable to a small animal model. This technique may useful to evaluate novel drugs, dosage and regiments for iron chelation therapy.

Keywords: β-thalassemic mice, liver, iron overload, deferiprone, MRI

Monitoring Hepatic Iron Content in Iron Overloaded β-Thalassemic Mice by Magnetic Resonance Imaging

Paranee Yatmark[1,*], Somkiat Hualjantug[2], Warida Jesdachest[2], Tararat Bunyanno[2], Kamonwat Surareungchai[2], Wuttiwong Teerapan[3], Saovaros Svasti[4], Suthat Fucharoen[4], Nopparwan Phumala Morales[1]

[1]Department of Pre-clinic and Applied animal science, Faculty of Veterinary Science, Mahidol University, Nakorn Pathom, Thailand.
[2]Department of Clinical Sciences and Public Health, Faculty of Veterinary Science, Mahidol University, Nakorn Pathom, Thailand.
[3]Department of Comparative science, Clinical Sciences, Faculty of Veterinary medicine, Kasetsart University, Bangkok, Thailand.
[4]Thalassemia Research Center, Institute of Molecular Biosciences, Mahidol University, Salaya Campus, Nakorn Pathom, Thailand.
[5]Department of Pharmacology, Faculty of Science, Mahidol University, Bangkok, Thailand.

*Email: paranee.yat@mahidol.edu**

Introduction

Increasing of hepatocellular carcinoma in patients with β-thalassemia has been recognized in the past few years. Iron overload is a major cause of this advance complication, therefore monitoring of hepatic iron is necessary for early diagnosis and evaluation of iron chelation therapy. Magnetic resonance imaging (MRI) is known as a useful non-invasive tool for monitoring hepatic iron overload in β-thalassemia patients. However, this technique is limit to a small animal model.

Objectives

MRI technique using T2*value was developed to study hepatic iron content and to monitor the effect of an iron chelator, deferiprone in b-thalassemic mice.

Quantitative T2 value by CMR2 software*

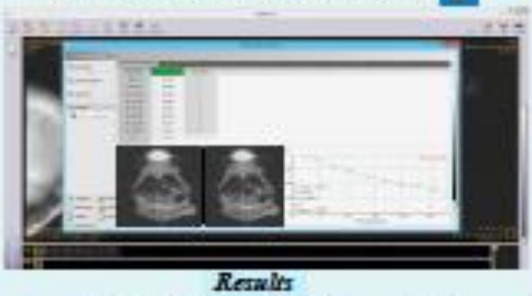

Materials and methods

Animals

Male and female heterozygous β-globin knockout mice (*hbb*$^{th3/+}$, BKO) 7 weeks of age and weighing 17-25 g were obtained from the Thalassemia Research Center, Institute of Science and Technology for Research and Development, Mahidol University, Thailand.

Group A: BKO mice :normal saline (0.9 % NaCl) (n=6)
Group B: BKO mice :iron dextran (20 mg/kg/day) (n=6)
Group C: BKO mice :iron dextran (20 mg/kg/day) + L1 (n=6)

MRI SCAN

Scanning by 1.5 T Siemens Magnetom
(Siemens AG, Medizinische Technik, Germany)

T2-weighted images

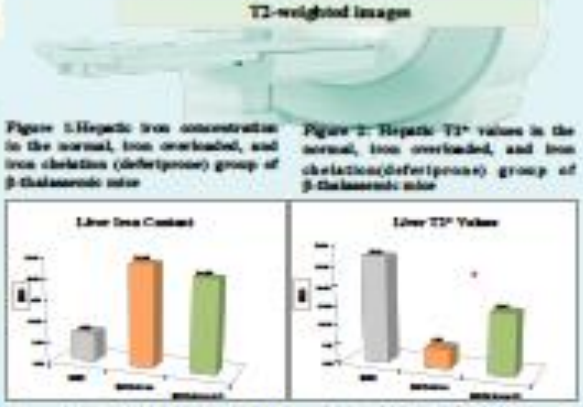

Figure 1.Hepatic iron concentration in the normal, iron overloaded, and iron chelation (deferiprone) group of β-thalassemic mice

Figure 2: Hepatic T2* values in the normal, iron overloaded, and iron chelation(deferiprone) group of β-thalassemic mice

Figure 3: T2-weighted images in the normal (a) and iron overloaded (b) group of β-thalassemic mice. T2-Weighted image showed hypointensity in the liver of iron overloaded group of β-thalassemic mice.

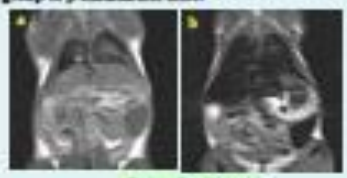

Results

This study demonstrated the markedly increased hepatic iron content in BKO mice after loading with iron dextran. Treatment with deferiprone significantly reduced iron deposition in the liver of BKO mice (Fig.1). In the iron overload group, T2* values was decreased to ms, corresponding with increased ferritin iron. Treatment of an iron chelation, deferiprone, T2* value was increased statistically significant difference from the iron overloaded group (Fig.2). T2-weighted image showed hypointensity in the liver of iron overloaded group of β-thalassemic mice (Fig.3). The values decreased to ms in corresponding with increased hepatic iron content in iron loaded β-thalassemic mice (r= and p=). Iron chelation with deferiprone, significantly increased liver T2* value to ms.

Statistical analysis was performed with SPSS software version 19.0

Conclusions

MRI-echo sequence allowed a good estimation of iron overload in liver of β-thalassemia mice. The results demonstrated that liver T2* values were decreased to ms for the iron overloaded thalassemic mice and correlated with iron overload status of the animals. In addition, liver T2* values increased in the group of the treatment of deferiprone, a ms. Iron estimation using the T2* CMR sequence is generally satisfactory and may help facilitate global access to tissue iron assessment. We suggested that T2* technique is good for monitoring hepatic iron overload in β-thalassemia mice model.

Acknowledgments

This study is supported by a grant from The Thailand Research Fund (MRG5980030). Deferiprone was kindly provided by The Government Pharmaceutical Organization, Bangkok, Thailand. The authors thank The Faculty of Veterinary Science, Mahidol University.